GA–A26459

THE BEHAVIOR OF INJECTED IMPURITIES UNDER RADIATING DIVERTOR CONDITIONS WITH PUFF-AND-PUMP TYPE PARTICLE CONTROL

by
T.W. PETRIE, G.D. PORTER, N.H. BROOKS, M.E. FENSTERMACHER, J.R. FERRON, A.W. HYATT, R.J. LA HAYE, C.J. LASNIER, A.W. LEONARD, T.C. LUCE, P.A. POLITZER, M.E. RENSINK, M.J. SCHAFFER, M.R. WADE, and J.G. WATKINS

JULY 2009

GENERAL ATOMICS

DISCLAIMER

GA–A26459

THE BEHAVIOR OF INJECTED IMPURITIES UNDER RADIATING DIVERTOR CONDITIONS WITH PUFF-AND-PUMP TYPE PARTICLE CONTROL

by
T.W. PETRIE, G.D. PORTER,* N.H. BROOKS, M.E. FENSTERMACHER,*
J.R. FERRON, A.W. HYATT, R.J. LA HAYE, C.J. LASNIER,* A.W. LEONARD,
T.C. LUCE, P.A. POLITZER, M.E. RENSINK,* M.J. SCHAFFER, M.R. WADE,
and J.G. WATKINS†

This is a preprint of a paper presented at the 36th EPS Conf. on Plasma Physics, in Sofia, Bulgaria, June 29th through July 3, 2009 and to be published in the *Proceedings.*

*Lawrence Livermore National Laboratory, Livermore, California.
†Sandia National Laboratories, Albuquerque, New Mexico.

Work supported by
the U.S. Department of Energy
under DE-FC02-04ER54698, DE-AC52-07N27344, and DE-AC04-94AL85000

GENERAL ATOMICS PROJECT 30200
JULY 2009

GENERAL ATOMICS

The Behavior of Injected Impurities under Radiating Divertor Conditions with Puff-and-Pump Type Particle Control

T.W. Petrie[1], G.D. Porter[2], N.H. Brooks[1], M.E. Fenstermacher[2], J.R. Ferron[1], M. Groth[2], A.W. Hyatt[1], R.J. La Haye[1], C.J. Lasnier[2], A.W. Leonard[1], T.C. Luce[1], P.A. Politzer[1], M.E. Rensink[2], M.J. Schaffer[1], M.R. Wade[1], and J.G. Watkins[3]

[1]*General Atomics, P.O. Box 85608, San Diego, California 92186-5608, USA*
[2]*Lawrence Livermore National Laboratory, Livermore, California 94550, USA*
[3]*Sandia National Laboratories, Albuquerque, New Mexico 87185, USA*

High values of heat exhaust at the divertor targets can be reduced by "seeding" the divertor with impurity particles, such that they radiate a significant fraction of the incoming power upstream of the divertor surfaces. Leakage of these impurities into the main plasma can be minimized by maintaining a strong flow of deuterium ions into the divertor through a combination of upstream deuterium gas puffing and active particle exhaust at the divertor targets, i.e., *puff-and-pump* [1]. Here we extend the successful application of this approach in [1] and show the importance of particle drifts to understanding this process.

Three cryopumps remove deuterium and argon atoms (Fig. 1). Argon was chosen as the injected seed impurity. Deuterium gas was introduced upstream of the divertor on the low-field side of the main plasma. The magnetic balance between divertors *dRsep* is characterized by the radial separation between primary and secondary separatrices at the outer midplane. In this study *dRsep* ranges from –1.5 cm (biased toward the lower divertor) to +1.5 cm (biased toward the upper divertor). We refer to configurations with $|dRsep| \geq$ 1 cm as single-null (SN), although the secondary null remains within the vacuum vessel. Reversing the direction of B_T changes the vertical direction of the ion $B \times \nabla B$ particle drift, $V_{\nabla B}$. Since this particle drift drives a poloidal convection of particles that strongly influences the global recirculation pattern of fuel particles between core and boundary, we find it physically meaningful to express results in terms of the ion $B \times \nabla B$ drift direction. We adopt the symbol $V_{\nabla B\uparrow}$ to cases in which the ion $B \times \nabla B$ drift is directed toward the top of the DIII-D vessel and $V_{\nabla B\downarrow}$ to those in which the ion $B \times \nabla B$ drift is directed toward the bottom of the vessel. When combined with the abbreviation lower single null (LSN) or upper single null (USN) describing the divertor geometry, the terms LSN-$V_{\nabla B\downarrow}$ or USN-$V_{\nabla B\downarrow}$ indicate the ion $B \times \nabla B$ drift drives flow from the core to the X-point in the former case and flow from the X-point to the core in the latter. Double-null (DN)-$V_{\nabla B\uparrow}$ indicates that the ion $B \times \nabla B$ drift drives flow from the lower X-point toward the upper X-point in a DN configuration.

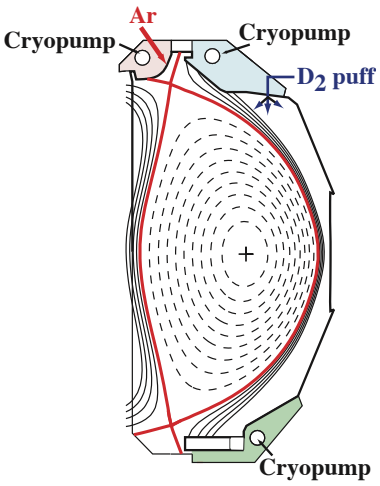

Fig. 1. Particle pumping and gas injection locations are shown together with the cross-section of a DN plasma.

Figure 2 shows the accumulation of argon inside upper-single-null, H-mode plasmas to be sensitive to the $V_{\nabla B}$ direction. In this comparison of USN-$V_{\nabla B\downarrow}$ and USN-$V_{\nabla B\uparrow}$ cases, argon was injected into the private flux region (PFR) of the upper divertor. Both had Γ_{D2} = 14.3 Pa m^3/s and a steady argon puff rate, Γ_{Ar}, of 0.13 Pa m^3/s [Fig. 2(a)]. Argon accumulation in the core was ≈3.5 times higher for $V_{\nabla B\uparrow}$ than for $V_{\nabla B\downarrow}$, as indicated by the

density of the dominant Ar^{16+} charge state $n_{Ar^{16+}}$ ($\approx n_{AR}$) at ρ=0.7 [Fig. 2(b)]. For similar discharges, analysis with the MIST [2] impurity transport code indicates that $n_{Ar^{16+}}$ should be >80% of n_{AR} at ρ=0.7 [1]. The rate at which argon was exhausted by the *upper outer* cryopump, $\Gamma_{P\text{-}Ar}$, was much higher for the $V_{VB\downarrow}$ case [Fig. 2(c)]: ≈85% of the injected argon was removed by the pump in the outer divertor for $V_{VB\downarrow}$ versus ≈35% for $V_{VB\uparrow}$.

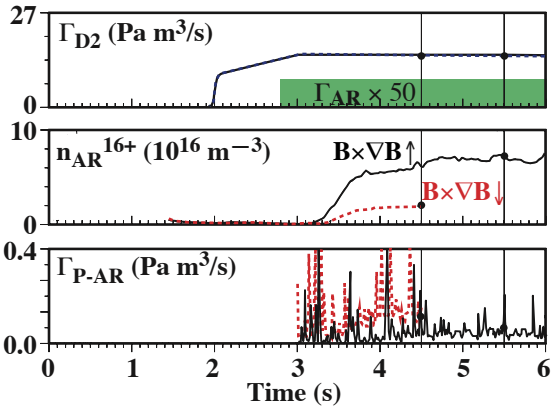

Fig. 2. The waveforms of (a) the deuterium and argon gas puff rates, (b) Argon 16^+ core density at ρ=0.7, and (c) argon exhaust are shown for USN-$V_{VB\uparrow}$ (solid) and USN-$V_{VB\downarrow}$ (dashed) cases.

Steady-state argon buildup in the core of SNs and DNs varies with Γ_{Ar} with constant Γ_{D2} (Fig. 3). In comparing *relative* argon accumula-tion, we define $\hat{n}_{Ar}$, which is taken as $\hat{n}_{Ar} = I_{ArXV}/n_e$ signal, where I_{ArXV} is the intensity of an ArXV line (22.14 nm) along a tangential chordal through the main plasma [1]. Argon was injected into the PFR of the *upper* divertor. Given the same Γ_{Ar}, the increase in $\hat{n}_{Ar}$ was roughly a factor of 3–4 larger than for DN-$V_{VB\downarrow}$ that in USN-$V_{VB\downarrow}$. Reversing the direction of $B \times \nabla B$ produced a ratio of $\hat{n}_{Ar}$ between the DN-$V_{VB\uparrow}$ and USN-$V_{VB\uparrow}$ cases of roughly two. In the DN-$V_{VB\uparrow}$ cases, however, $\hat{n}_{Ar}$ was almost twice that in the DN- $V_{VB\downarrow}$ cases.

The effectiveness in reducing $\hat{n}_{Ar}$ by raising the D_2 injection rate depends on plasma configuration and V_{VB} direction. With Γ_{Ar} constant, we determine how $\hat{n}_{Ar}$ varies with Γ_{D2} for the four cases shown in Fig. 4. Again, argon was injected into the PFR of the upper divertor. In all cases, $\hat{n}_{Ar}$ decreased when Γ_{D2} was increased from 5 Pa m^3/s to 10 Pa m^3/s. At higher Γ_{D2}, $\hat{n}_{Ar}$ continued to decrease in only the USN-$V_{VB\downarrow}$ case. The $\hat{n}_{Ar}$ was comparable for DN-$V_{VB\downarrow}$ and USN-$V_{VB\downarrow}$ when $\Gamma_{D2} \le 10$ Pa m^3/s, but diverged when Γ_{D2} was raised to 13 Pa m^3/s. At this level of Γ_{D2} for the DN-$V_{VB\downarrow}$ case, the inner divertor leg was tenuously attached, with $n_e \le 1\times10^{19}$ m^{-3} and $T_e \le 10$ eV. For USN-$V_{VB\downarrow}$, on the other hand, the inner divertor remained firmly attached, with $n_e \approx 10^{20}$ m^{-3} and $T_e =$ 10–20 eV.

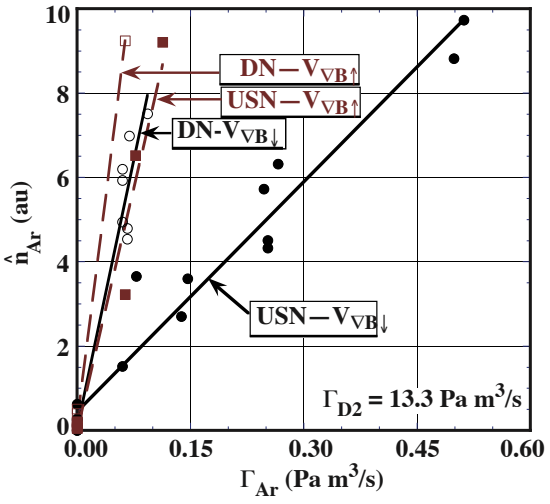

Fig. 3. Relative argon core accumulation $\hat{n}_{Ar}$ in upper SN and DN plasmas vs argon injection rate for both $V_{VB\uparrow}$ and $V_{VB\downarrow}$ cases. Linear fits to the data for each case are included. Argon was injected into the upper divertor PFR.

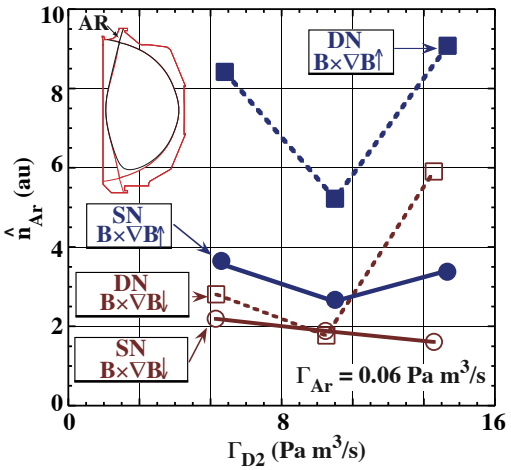

Fig. 4. Relative argon core accumulation $\hat{n}_{Ar}$ in upper SN and DN plasmas is plotted vs the deuterium injection rate for both $V_{VB\uparrow}$ and $V_{VB\downarrow}$.

Because the mean-free path of neutral argon in the upper inner divertor region was at least an order of magnitude larger for the $V_{VB\downarrow}$ case, the escape of neutral argon from the upper inner leg to the high-field side SOL was much more likely for DN-$V_{VB\downarrow}$ than for USN-$V_{VB\downarrow}$.

To ascertain at what point the behavior of impurities in DNs begins to resemble that in SN plasmas, we vary *dRsep* shot-to-shot, holding both Γ_{D2} and Γ_{Ar} constant. While n_{PED} remained fairly steady [Fig. 5(a)], $\hat{n}_{Ar}$ decreased by a factor of three between *dRsep* = 0.0 and +0.5 cm, with little change in $\hat{n}_{Ar}$ beyond that [Fig. 5(b)]. The greatest change in $\hat{n}_{Ar}$ occurred near *dRsep* ≈ +0.4 cm. The energy confinement was similar for both *dRsep* = 0 and *dRsep* = +0.5 cm cases, and so was unlikely causing the change in $\hat{n}_{Ar}$. The recycling light near the upper inner target, $D_{\alpha\text{-IN}}$ jumped between *dRsep* = +0.3 cm and +0.5 cm, but varied little with further increase, suggesting that full attachment at the inner target characteristic of USN-$V_{VB\downarrow}$ plasmas had largely been established for *dRsep* > +0.5 cm [Fig. 5(c)]. For shots like those in Fig. 5, the e-folding scrape-off width of the parallel heat flux density at the outer midplane was also 0.4–0.5 cm [3]. Hence, with *dRsep* ≥ +0.4 cm, significant power from the low-field side SOL can reach the high field side target and maintain density and temperature high enough to impede the escape of neutral argon to the high field side SOL. Increasing *dRsep* further leads only to a marginal increase in power reaching the inner target and in the intensity of recycling there.

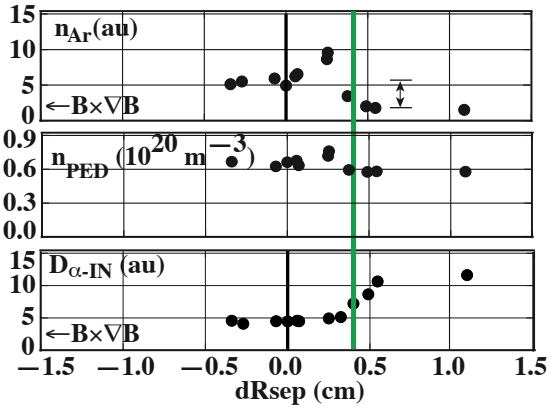

Fig. 5. (a) Relative argon core accumulation $\hat{n}_{Ar}$, (b) electron pedestal density, and (c) $D_{\alpha\text{-IN}}$ are shown vs *dRsep*. Argon was injected into the upper divertor PFR. The solid vertical line is the approximate transition from DN-to-SN behavior during puff-and-pump; Γ_{D2} = 13.3 Pa m^3/s and Γ_{Ar} = 0.06 Pa m^3/s.

The effect of particle drifts [4] in the SOL and divertor plasmas is crucial to understanding the experimental results presented above. The UEDGE fluid transport code [5], which includes a full particle drift package [6] applicable to H-mode, magnetically unbalanced plasmas, is used to evaluate the complex behavior resulting from the interaction of these multiple drifts. Based on UEDGE modeling of the two plasmas shown in Fig. 2, we identify the $E_r \times B$ drift as particularly important. The radial electric field E_r is largely determined by the electron temperature gradient normal to the local flux surfaces. UEDGE shows that this drift preferentially sweeps much of the injected argon ionized in the PFR toward the *inner* divertor target for USN-$V_{VB\uparrow}$, and toward the *outer* target for USN-$V_{VB\downarrow}$. In the $V_{VB\uparrow}$ case, UEDGE predicts an increase in argon at the inner target that would enhance the local radiated power near the inner target; at an elevated argon concentration, this would lead to a detached *inner* divertor leg, as occurred in Fig. 2 for $V_{VB\uparrow}$. For $V_{VB\downarrow}$, UEDGE analysis indicates that the injected argon is preferentially swept away from the inner divertor target toward the *outer* target. Although electron temperature and peak heat flux were reduced at the outer divertor target, detachment of this leg from the divertor target did not occur at the Γ_{D2} and perturbing Γ_{Ar} used here. In fact, the electron temperature at the *inner* divertor separatrix target was virtually unchanged, even when Γ_{Ar} was raised to perturbing levels and was likely related to sweeping the injected argon away from the inner divertor target for the $V_{VB\downarrow}$ cases. The impact of the $E_r \times B$ drift on the argon distribution at the outer

divertor target is reflected by the UEDGE prediction that the argon exhaust rate by the outer divertor cryopump is two-and-half times higher for USN-$V_{\nabla B\downarrow}$ than USN-$V_{\nabla B\uparrow}$. This is consistent with experiment. UEDGE predicts that the primary role of the deuterium puff is to alter the structure of the SOL electric fields, and thus the plasma flow from drifts. The effect of the deuterium parallel flow on entrainment of argon is secondary. UEDGE predicts that the ratio of argon accumulation in the core for $V_{\nabla B\uparrow}$ to that for $V_{\nabla B\downarrow}$, ($n_{\text{AR-}\nabla\text{B}\uparrow}/n_{\text{AR-}\nabla\text{B}\downarrow}$), is ≈3.5/1 from experiment versus ≈10/1 from the UEDGE prediction for the 90% poloidal flux surface inside the main plasma. Uncertainty in the details involved in the argon transport, e.g., ELMs, makes only a qualitative agreement between UEDGE modeling and experiment possible. Figure 3 shows that argon accumulation in the main plasma of DNs was greater than that in comparable SNs with the same $V_{\nabla B}$ direction, again in qualitative agreement with UEDGE predictions. When $V_{\nabla B}$ was directed toward the *upper* divertor, ($n_{\text{AR-}\nabla\text{B}\uparrow\text{-DN}}/n_{\text{AR-}\nabla\text{B}\uparrow\text{-USN}}$) ≈ 2 from experiment and ≈2.3 from UEDGE at the 90% poloidal flux. For the cases where $V_{\nabla B}$ was directed toward the *lower* divertor but with argon still injected into the upper divertor, ($n_{\text{AR-}\nabla\text{B}\downarrow\text{-DN}}/n_{\text{AR-}\nabla\text{B}\downarrow\text{-USN}}$) ≈ 3.3 from experiment and ≈3.4 from UEDGE.

While the same particle drifts are in play for both DNs and SNs, DNs differ in important ways from SNs. Power flows out of the core plasma primarily on the low field side [3], with roughly half of this SOL-transported power, in principle, available for maintaining plasma attachment at the inboard target of a SN. However, in a DN, power flowing into the SOL on the low-field side is shunted to the two outer divertor targets, starving the inner divertor targets of the power needed to maintain plasma ionization. Thus, the characteristic electron temperature for the inboard SOL plasma of a DN is always less than that of a comparable SN. In addition, the SOL density profile on the high field side of DNs is also narrower compared with that of comparable SNs [7]. Since both upper and lower inner divertor targets are only tenuously attached (and sometimes detached) in DNs, it is easier for argon neutrals to leak out of the upper divertor into the SOL on the high field side.

Increasing Γ_{D2} for USN-$V_{\nabla B\downarrow}$ cases reduced the leakage of argon out of the divertor and its subsequent buildup inside the plasma. However, increasing Γ_{D2} was much less effective in this regard for the USN-$V_{\nabla B\uparrow}$ cases, and this may be the result of the cooling and possible partial detachment of the inner target, making escape of the argon from the divertor (and its subsequent accumulation in the main plasma) easier. For DNs, the puff-and-pump solution was least effective. Gas puffing from the low-field side of the DN enhanced the deuterium flow into the two divertors on the low-field side, but not into the high-field side divertors, since the high-field SOL is severed magnetically from the low-field SOL in DN. Because particle removal rates of argon by both outer divertor pumps depend strongly on the direction of $V_{\nabla B}$, values of Γ_{D2} leading to effective containment of impurities for one divertor is not likely to be as successful in the other divertor.

This work was supported by the US Department of Energy under DE-FC02-04ER54698, DE-AC52-07NA27344, and DE-AC04-94ER85000.

References

[1] T.W. Petrie, et al., J. Nucl. Mater. **363-365** (2007) 416 (*and references therein*).
[2] R.A. Hulse, Nucl. Technol. Fusion **3** (1989) 259.
[3] T.W. Petrie, et al., J. Nucl. Mater. **290-293** (2001) 935.
[4] A.V. Chankin, J. Nucl. Mater. **241-243** (1997) 199.
[5] T.D. Rognlien, et al., J. Nucl. Mater. **196-198** (1992) 347.
[6] T.D. Rognlien, et al., J. Nucl. Mater. **266-269** (1999) 654.
[7] T.W. Petrie, et al., J. Nucl. Mater. **313-316** (2003) 834.